Experimental and theoretical study of the hyperfine structure in the $4f^7 5d6s6p$ configuration of Gd I

H.-D. Kronfeldt, G. Klemz, and S. Kröger
Optisches Institut, Technische Universität Berlin, Hardenbergstrasse 36, 10623 Berlin, Germany

J.-F. Wyart
Laboratoire Aimé Cotton, CNRS II, Centre Universitaire, Bâtiment 505, 91405 Orsay, France

(Received 22 February 1993)

A parametric hyperfine-structure (hfs) analysis of 24 excited even-parity levels of the $4f^7 5d6s6p$ configuration in Gd I was performed. The interpretation has been carried out based on a refined multiconfigurational fine-structure (fs) calculation taking altogether 177 assignments into account. The set of fs parameters as well as the leading eigenvector percentages of levels relevant for this paper are given. SL-limit effective-operator expressions are presented for the magnetic-dipole and electric-quadrupole hfs of arbitrary states built from four open electron shells. The following single-electron hfs parameters a^{10}_{6s} and b^{02}_{6p} were deduced for ^{155}Gd, $a^{10}_{6s} = -1270(22)$ MHz, $b^{02}_{6p} = 1507(26)$ MHz and for ^{157}Gd, $a^{10}_{6s} = -1668(28)$ MHz, $b^{02}_{6p} = 1603(29)$ MHz. For the odd-parity level $4f^7 5d6s^2\ ^7D_4$ the magnetic-dipole A and electric-quadrupole B hfs constants were found to be $^{155}A = -11.3(2.1)$ MHz, $^{155}B = 54(9)$ MHz, $^{157}A = -14.8(2.7)$ MHz, and $^{157}B = 58(10)$ MHz. The validity of all single-electron hfs parameters was checked using general trends of the corresponding $\langle r^{-3}\rangle^{k_s k_l}_{nl}$ values known for the series of the lanthanides. Finally, the evaluation of the electric nuclear quadrupole moment is discussed.

PACS number(s): 32.30.Jc, 35.10.Fk, 31.30.Gs

I. INTRODUCTION

Numerous investigations of the hyperfine structure (hfs) of lanthanides have been conducted recently. Effective $\langle r^{-3}\rangle$ values obtained from the corresponding radial hfs parameters and the nuclear moments have been determined for several configurations, thereby allowing the possibility of systematic comparisons. A comprehensive summary of known results is found in [1]. However, only parametric analyses for configurations with up to three open electron shells have been completed [2]. Configurations of the type $4f^n 5d6s6p$ — with four open electron shells — have not been parametrized, although they are present in almost all lanthanides [3].

Furthermore several high-resolution measurements of hfs and isotope-shift (IS) effects in Gd have been performed by various groups on the neutral atom [2, 4–13] and on singly ionized Gd [14] in the past few years. The investigated transitions in Gd I connect low-lying odd levels of configurations of the type $4f^7(5d+6s)^3$ with those of $4f^7 5d6s6p$, i.e., a configuration with four open electron shells. Experimental magnetic-dipole and electric-quadrupole constants A and B for this configuration of Gd I are well established for altogether 24 levels between 16 886 cm^{-1} and 25 661 cm^{-1} especially, with our present measurements and those reported in [2, 6–9, 11]. However, due to lack of existing fine-structure (fs) calculations, no decomposition into the one-electron hfs parameters a_{nl} and b_{nl} could be carried out up to now. Thus only a qualitative discussion regarding measured trends of the J dependence of the hfs constants within two terms was presented by [11] giving some hints of the mixing with other states.

To obtain the eigenvector percentages of the even levels required for such a decomposition, fs calculations have been performed for the three configurations $4f^7 6s^2 6p$, $4f^7 5d6s6p$, and $4f^7 5d^2 6p$ with the use of the chain of computer programs developed at the Laboratoire Aimé Cotton in Orsay [15].

With the use of calculated wave functions, the experimental hfs constants A and B, and explicit expressions for the angular parts of the hfs matrix elements, we have performed a parametric hfs analysis for a configuration with four open electron shells. The explicit expressions are given in the Appendix.

II. EXPERIMENTAL PROCEDURE AND INVESTIGATIONS

Laser-induced resonance fluorescence in an atomic beam was used in our experimental setup as already described in Refs. [8] and [12]. Furthermore, a self-developed demountable hollow cathode was used for intermodulated optogalvanic spectroscopy [16] on the first three spectral lines listed below. In the present IS investigations the following optical transitions of type $4f^7 5d6s^2 \rightarrow 4f^7 5d6s6p$ yielded additional even-level hfs constants: 629.287 nm ($^9D^o_5 \rightarrow\ ^{11}D_5$), 640.855 nm ($^9D^o_6 \rightarrow\ ^{11}D_6$), 613.502 nm ($^9D^o_6 \rightarrow\ ^{11}D_7$), 569.249 nm ($^7D^o_3 \rightarrow\ ^7D_4$), 563.099 nm ($^7D^o_4 \rightarrow\ ^7D_4$), 572.776 nm ($^7D^o_5 \rightarrow\ ^9F_6$), and 586.958 nm ($^7D^o_3 \rightarrow\ ^7P_2$). As a representative example, the spectrum of the weak 586.958 nm transition is shown in Fig. 1. This previously untabulated transition was observed here. Further, transitions of the type $4f^7 5d^2 6s \rightarrow 4f^7 5d6s6p$ 576.976 nm ($^{11}F^o_5 \rightarrow\ ^9F_6$), 589.806 nm ($^{11}F^o_6 \rightarrow\ ^9F_6$), 606.514 nm ($^{11}F^o_7 \rightarrow\ ^9F_6$),

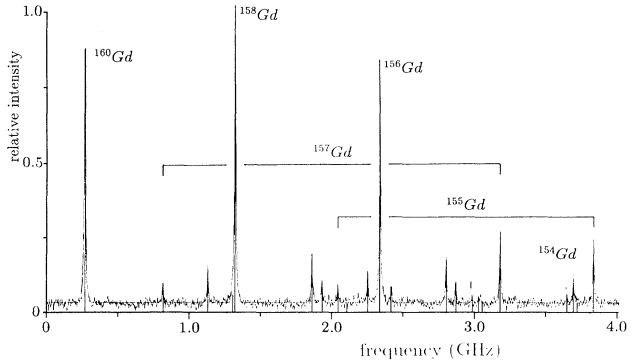

FIG. 1. Spectrum of Gd I $\lambda = 586.958$ nm, $4f^7 5d6s^2\ {}^7D_3^o \rightarrow 4f^7 5d6s6p\ {}^7P_2$, obtained using the atomic beam apparatus. The fluorescence was observed through an interference filter at 406 nm.

563.198 nm ($^{11}F_5^o \rightarrow {}^9G_6$), 575.417 nm ($^{11}F_6^o \rightarrow {}^9G_6$), and 591.307 nm ($^{11}F_7^o \rightarrow {}^9G_6$) were measured — the last one also being an untabulated transition.

The hfs constants of the lower levels agree well with those reported in [2] and [17]. For $^7D_4^o$ there are no prior values. We found

$$^{155}A(^7D_4^o) = -11.3(2.1)\ \text{MHz}\ ,$$

$$^{155}B(^7D_4^o) = 54(9)\ \text{MHz}\ ,$$

$$^{157}A(^7D_4^o) = -14.8(2.7)\ \text{MHz}\ ,$$

$$^{157}B(^7D_4^o) = 58(10)\ \text{MHz}\ .$$

In Table I our present and all known experimental hfs constants taken from [2, 6–9, 11] of 24 excited even-parity levels of $4f^7 5d6s6p$ and their mean values are compiled. Data from [6] were not considered when calculating the mean, owing to excessive scattering of the isotopic ratios $^{157}B/^{155}B$ and $^{157}A/^{155}A$ resulting from the stated values. For example, one obtains for the states at 17 749.978 cm^{-1}, 18 070.257 cm^{-1}, 18 083.642 cm^{-1}, and 18 509.198 cm^{-1} the B ratios 0.42(9), 1.35, 0.90(4), and 0.89, respectively, which are far off the values 1.065 34(3) determined by Unsworth [17] with atomic-beam magnetic resonance and 1.065 31(13) by Childs [2], who employed laser rf double resonance spectroscopy. Similarly, the A ratios for the levels 17 973.611 cm^{-1} and 18 509.198 cm^{-1} with 1.58 and 1.25 do not aggree with 1.311 43(23) [17] and 1.312 67(35) [2]. The hyperfine splitting constants given in [6] for the ground term $4f^7 5d6s^2\ {}^9D$ are also not in complete accord with the results of Unsworth. Nevertheless, their excited-state splitting constants are given here for the sake of completeness.

III. FINE STRUCTURE

The first fine structure fit was carried out by Nir [18] as early as 1969. He regarded the group of configurations $[4f^7(^8S)6s^2 6p + 4f^7(^8S)5d6s6p + 4f^7(^8S)5d^2 6p]$ (see Fig. 2). When further experimental data became available, calculations in the configurations $4f^7 5d6s6p$ and $4f^7 5d^2 6p$ were performed by van Kleef, Blaise, and Wyart [19]. They came to the conclusion of non-negligible interaction also with the levels of the $4f^8 5d6s$ and $4f^7 6s^2 np$ ($n = 6, 7, 8$) configurations to interpret the fine-structure levels satisfactorily. So it became necessary for us to perform an extended fs analysis. It is based on the subconfigurations $[4f^7(^8S + {}^6P)6s^2 6p + 4f^7(^8S + {}^6P)5d6s6p + 4f^7(^8S)5d^2 6p]$, i.e., the ^6P core was additionally taken into account. Actually, even-parity levels of Gd I built on $4f^7(^6P)$ are still unidentified, but the fine-structure study of the core configuration $4f^7$ reveals that $^6P_{7/2}$ is, by far, the largest "small" component in the eigenfunction of the isolated ground level $^8S_{7/2}$. So, we could expect from the present calculations a significant improvement of the eigenfunctions for the lowest even energy levels. The levels for which the hyperfine-structure splitting is to be parametrized are within the interval 16 886 cm^{-1} – 25 376 cm^{-1}. Thus one expects only a minor influence on the subsequent hfs analysis by neglecting the interaction between the calculated group of configurations and the configuration $4f^8 5d6s$, whose lowest level is a $^9G_7$ state at 24 255.103 cm^{-1}. Therefore a separate calculation of $4f^8 5d6s$ should be sufficient for our purpose. Introduction of the remaining low-lying configuration $4f^8(^7F)6s^2$, which forms only one term ^7F, would increase the amount of additional parameters disproportionately and at the present stage of the studies in the end might produce more difficulties with the quality of the fit.

For the fs calculation we formed SL-coupled basis states according to one of the following four schemes for each of the individual configurations involved:

$$|\,[4f^7(S_1L_1)6s^2 6p]SLJ\rangle\ , \qquad (1)$$

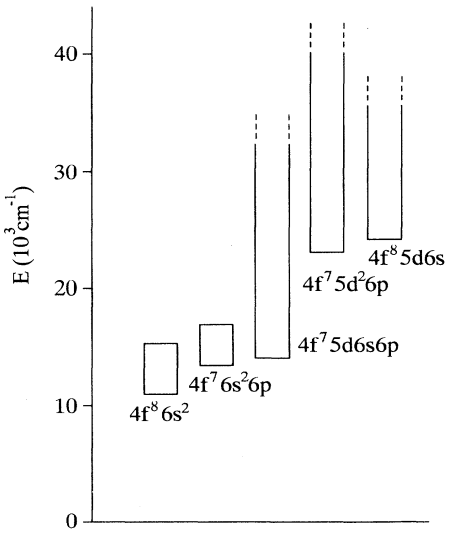

FIG. 2. Energy levels of the even configurations of Gd I. The vertical lines represent the energy intervals which are covered by the known levels of a configuration. Dashed lines indicate regions of existing but yet undiscovered or unassigned levels of a configuration.

$$|\{[4f^7(S_1L_1)5d](S_{12}L_{12})[6s6p](S_{34}L_{34})\}SLJ\rangle\ , \quad (2)$$

$$|\{[4f^7(S_1L_1)5d^2(S_2L_2)](S_{12}L_{12})6p\}SLJ\rangle\ , \quad (3)$$

$$|\{[4f^8(S_1L_1)5d](S_{12}L_{12})6s\}SLJ\rangle\ . \quad (4)$$

177 assignments are known for the group $4f^7(5d+6s)^26p$ and 66 for $4f^85d6s$ according to [3]. The fit was carried out with 41 Slater parameters for the mixed configurations and 10 parameters for the single configuration. Of those 41 parameters 24 were free to vary and the remaining were held by means of constraints detailed in Table II. The parameters are given in the first column; the values of the radial parameters and the associated standard

TABLE I. Experimental hyperfine splitting constants A and B. If more than one value is given for an individual level its mean is taken (slanted) and the stated experimental uncertainties are one times the standard deviation. E_0: the observed energy of the upper level belonging to the even-parity configuration $4f^75d6s6p$. The present work is denoted by the relevant wavelength in the Reference column at which a measured transition connects the given upper energy level. Values labeled by an asterisk were excluded in the calculation of the mean owing to inconsistencies in comparison with the results given by other authors as explained in the text.

Level E_0 (cm^{-1})	Assignment	J	^{155}Gd A_{expt} (MHz)	^{155}Gd B_{expt} (MHz)	^{157}Gd A_{expt} (MHz)	^{157}Gd B_{expt} (MHz)	Reference
16 885.739	^{11}D	5	-111.18(24)	242(8)	-145.8(3)	258(5)	629.287 nm
17 318.942		6	-106(3)	290(8)	-140(4)	309(8)	640.855 nm
18 014.403		7	-109.7(2)	-53.9(6)	-143.9(2)	-57.5(6)	613.502 nm
17 227.969	^{9}F	1			352*	87.7*	[6]
			266.67(24)	76.2(6)	350.03(23)	78.9(6)	[7]
			264.1(1.4)	77.3(11)	344.18(37)	81.3(5)	[11]
			265.4(1.8)	*76.75(77)*	*347.1(4.1)*	*80.1(1.7)*	
17 380.827		2	73(5)*	-323.0(1.0)*	98.0(8)*	-349(4)*	[6]
			72.97(19)	-328.7(1.0)	96.17(20)	-353.7(1.0)	[7]
			72.54(19)	-327.7(2.3)	95.1(3)	-349.1(2.4)	[8]
			73.15(14)	-328.62(74)	95.73(14)	-350.03(76)	[9]
			72.87(62)	-329.3(2.0)	95.56(47)	-348.5(1.3)	[11]
			72.88(26)	*-328.58(66)*	*95.64(44)*	*-350.3(2.3)*	
17 617.767		3	31.1(4)*	-391(1)*	41.1(3)*	-423(3)*	[6]
			31.66(18)	-395.8(1.8)	41.27(20)	-415.4(1.9)	[7]
			31.5(3)	-393.2(1.8)	41.3(4)	-418.9(1.9)	[8]
			31.20(10)	-393.66(92)	40.92(10)	-420.00(94)	[9]
			30.91(44)	-392.2(2.9)	40.90(39)	-417.8(2.2)	[11]
			31.32(33)	*-393.7(1.5)*	*41.10(22)*	*-418.0(2.0)*	
17 973.611		4	-4.87*	-283*	-7.68*	-303*	[6]
			-4.95(23)	-288.3(3.1)	-6.51(26)	-304.0(3.3)	[7]
			-5.9(5)	-273.8(3.3)	-7.7(6)	-291.7(3.5)	[8]
			-5.22(38)	-284.6(4.1)	-6.80(27)	-305.7(2.1)	[11]
			-5.36(49)	*-282.2(7.5)*	*-7.00(62)*	*-300.5(7.6)*	
18 509.198		5	7.07*	-96.4*	8.83*	-86.2*	[6]
			6.08(21)	-86.6(3.9)	7.89(6)	-91.9(1.1)	[7]
			5.91(52)	-88.5(5.5)	7.73(43)	-94.8(4.6)	[11]
			6.00(12)	*-87.6(1.3)*	*7.81(11)*	*-93.4(2.1)*	
17 749.978	^{9}D	2	-88.7(1)*	-21.2(1.1)*	-117(3)*	-8.96(1.36)*	[6]
			-86.63(11)	-21.6(8)	-114.97(15)	-23.3(1.1)	[7]
			-87.0(6)	-20.6(3.7)	-114.47(50)	-21.9(3.9)	[8]
			-87.30(15)	-22.51(81)	-114.84(14)	-24.05(78)	[9]
			-86.94(76)	-23.4(2.8)	-113.98(69)	-25.2(2.6)	[11]
			-86.97(27)	*-22.0(1.2)*	*-114.47(50)*	*-23.6(1.4)*	
17 795.267		3	-94.7(1)*	162.0(1.0)*	-125(1)*	162(1)*	[6]
			-93.97(23)	160.2(2.4)	-123.52(31)	169.7(2.9)	[7]
			-94.1(7)	149.9(2.1)	-123.4(9)	159.6(2.2)	[8]
			-93.96(10)	151.68(1.16)	-123.80(11)	162.60(98)	[9]
			-94.30(50)	154.7(3.1)	-123.35(53)	163.2(3.2)	[11]
			-94.08(19)	*154.1(4.5)*	*-123.52(20)*	*163.8(4.3)*	
17 930.516		4	-72.1(1)*	205(3)*	-94.8(1)*	220(4)*	[6]
			-70.86(41)	229.1(5.2)*	-91.46(35)	238.1(6.1)*	[7]
			-71.3(2)	206.6(3.2)	-93.5(3)	220.1(3.5)	[8]
			-71.47(7)	205.26(96)	-93.45(8)	220.67(93)	[9]
			-72.17(23)	207.8(1.9)	-94.27(36)	220.8(2.9)	[11]
			-71.45(54)	*206.6(1.3)*	*-93.2(1.2)*	*220.52(37)*	
18 070.257		6	-101*	-59.4*	-134*	-80.2*	[6]
			-101.86(9)	-61.6(2.1)	-133.76(7)	-65.8(1.7)	[7]
			-101.67(10)	-60.9(5.4)	-133.33(8)	-64.9(5.8)	[8]
			-101.48(46)	-60.5(5.7)	-133.28(35)	-64.1(4.4)	[11]
			-101.67(19)	*-61.00(56)*	*-133.46(26)*	*-64.93(85)*	

TABLE I *(Continued).*

Level E_o (cm^{-1})	Assignment	J	^{155}Gd A_{expt} (MHz)	^{155}Gd B_{expt} (MHz)	^{157}Gd A_{expt} (MHz)	^{157}Gd B_{expt} (MHz)	Reference
18 083.642		5	-97.8(1)*	107(2)*	-132(2)*	96.6(21)*	[6]
			-98.63(23)	106.8(4.0)	-129.32(1)	112.9(5)	[7]
			-98.5(4)	110.7(4.9)	-129.2(6)	117.9(5.2)	[8]
			-98.36(26	108.7(2.4)	-129.44(27)	114.9(2.8)	[11]
			-98.50(14)	*108.7(2.0)*	*-129.32(12)*	*115.2(2.5)*	
23 103.660	^9F	1	136.3(1.0)	59(8)	174.6(1.0)	65(8)	[2]
23 215.028		2	28.4(4)	-219(8)	38.0(4)	-233(8)	[2]
23 389.782		3	2.3(4)	-295(8)	2.3(4)	-312(8)	[2]
23 644.156		4	-7.6(4)	-248(8)	-9.2(4)	-266(8)	[2]
23 999.912		5	-10.6(4)	-78(8)	-13.6(4)	-80(8)	[2]
24 430.425		6	-41.45(2)	351.9(5.4)	-54.36(2)	374.9(5.8)	572.776 nm
			-41.54(15)	342.3(1.4)	-54.48(20)	364.6(1.5)	606.514 nm
			-41.27(31)	353.8(4.8)	-54.1(4)	376.9(5.1)	589.806 nm
			-41.79(21)	342(8)	-54.8(3)	364.9(7.7)	576.976 nm
			-41.52(22)	*348(6)*	*-54.4(3)*	*370(6)*	
25 376.313		7	-6.7(4)	592(8)	-8.5(4)	632(8)	[2]
24 458.988	^7P	2	239.3(4)	-4(8)	313.7(4)	-4(8)	[2]
			239.30(56)	-4.6(1.6)	313.82(74)	-4.9(1.7)	586.958 nm
			-239.30(48)	*-4.30(39)*	*313.76(8)*	*-4.43(40)*	
24 849.514	^9D	4	-39.9 (4)	103(8)	-52.5 (4)	102(8)	[2]
24 988.884	^7D	4	39.9(1.7)	289(16)	52.3(2.2)	308(17)	569.249 nm
			36.3(1.4)	295(16)	47.9(1.9)	313(19)	563.099 nm
			38.1(2.5)	*292(5)*	*50.1(3.1)*	*310(4)*	
25 043.649	^9D	5	-28.9(4)	412(8)	-37.9(4)	439(8)	[2]
24 854.297	$^9G^a$	6	-72.5(4)	521(8)	-95.0(4)	555(8)	[2]
			-72.39(14)	526(4)	-95.97(19)	560(4)	591.307 nm
			-72.74(11)	534.6(1.9)	-95.38(14)	569.5(2.0)	575.417 nm
			-72.86(10)	526.9(7)	-95.48(10)	561.3(0.8)	563.198 nm
			-72.62(22)	*527(6)*	*-95.46(40)*	*561(6)*	

[a] $4f^8 5d6s$.

deviations appear in the following three colums. At the end of the table the standard deviation is given as defined by Racah

$$\langle \overline{\delta E} \rangle = \left[\sum (E_o - E_c)^2 / (N - p) \right]^{1/2} .$$

E_o is the observed, E_c the calculated value of the levels, N is the number of observed levels, and p is the number of parameters which have been used. The calculations have been carried out by means of four programs [15].

Regarding the $4f^8 5d6s$ configuration, some parameter values deviated from the regular trends in neutral lanthanides [20] and especially the spin-orbit parameter ζ_{5d} turned out to be substantially smaller than expected. We ascribe the poor quality of the fit to a perturbation by upper subconfigurations of $4f^8 5d6s$, the present study being limited to the parent ^7F term of $4f^8$. Thus we omitted the parameter set of $4f^8 5d6s$ in Table II.

Our analysis leads in one case to a new designation: the level at 23 103.660 cm^{-1} belongs predominantly to $4f^7 5d6s6p\,{}^9F_1$ instead of $4f^7 5d^2 6p\,{}^{11}G_1$ according to [3]. In Table III the leading eigenvector percentages of the levels relevant to our hyperfine investigation are listed. These levels have the common feature of belonging predominantly ($\approx 98\%$) to the configuration $4f^7 5d6s6p$, although their leading eigenvector component is in most cases only 50 – 80 %. In particular, the level at 24 849.514 cm^{-1} arises only 31.04% from the $^9D_4$ state. So, without loss of significance in the hfs analysis, we neglected the contributions of the configurations $4f^7 6s^2 6p$ and $4f^7 5d^2 6p$ to the levels of Table III. Only the state at 17 749.978 cm^{-1} with a 10.16% perturbation by $4f^7 6s^2 6p$ needs special treatment.

IV. HYPERFINE STRUCTURE ANALYSIS

In Table IV the measured magnetic and electric hfs constants A and B known so far are compiled for altogether 24 levels. Using the effective-operator technique [21] the experimental hfs constants A_{expt} and B_{expt} of $4f^7(^8S + {}^6P)5d6s6p$ can be expanded into the following expressions:

$$\begin{aligned} A_{expt} = \; & \alpha^{10}_{4f}(J) a^{10}_{4f} + \alpha^{01}_{4f}(J) a^{01}_{4f} + \alpha^{12}_{4f}(J) a^{12}_{4f} \\ & + \alpha^{10}_{5d}(J) a^{10}_{5d} + \alpha^{01}_{5d}(J) a^{01}_{5d} + \alpha^{12}_{5d}(J) a^{12}_{5d} \\ & + \alpha^{10}_{6s}(J) a^{10}_{6s} \\ & + \alpha^{10}_{6p}(J) a^{10}_{6p} + \alpha^{01}_{6p}(J) a^{01}_{6p} + \alpha^{12}_{6p}(J) a^{12}_{6p} , \end{aligned} \quad (5)$$

$$B_{\text{expt}} = \beta_{4f}^{11}(J)b_{4f}^{11} + \beta_{5d}^{02}(J)b_{5d}^{02} + \beta_{5d}^{13}(J)b_{5d}^{13} + \beta_{5d}^{11}(J)b_{5d}^{11} + \beta_{6p}^{02}(J)b_{6p}^{02} + \beta_{6p}^{11}(J)b_{6p}^{11} \,. \quad (6)$$

The $a_{nl}^{k_s k_l}$ and $b_{nl}^{k_s k_l}$ are the standard relativistic one-electron hfs parameters. The superscript denotes the rank k_s in spin space and k_l in orbital space of the corresponding tensor operator comprising part of the hyperfine Hamiltonian for electron configurations of the type nl^N [21, 24]. $\alpha_{nl}^{k_s k_l}$ and $\beta_{nl}^{k_s k_l}$ are the related angular coefficients and can be calculated by the methods of Racah algebra alone, provided the states are pure. In our case, however, one has to consider in addition the admixtures as given by the fs analysis. For the decomposition into the one-electron parameters it was necessary to derive general expressions from the effective hfs Hamiltonian for the A and B values of SL-coupled states built from four open electron shells. These expressions are reproduced in the Appendix. States of such configurations are present in almost all lanthanides and will certainly be studied in the future.

The experimental hfs parameters were then estimated by a least-squares fit procedure to a set of linear equations of types (5) and (6). Due to strong linear correlations the number of parameters had to be reduced using Casimir's

TABLE II. Slater parameters for the even-parity subconfigurations $[4f^7(^8S+{}^6P)6s^26p + 4f^7(^8S+{}^6P)5d6s6p + 4f^7(^8S)5d^26p]$. f, the parameter has not been changed during the last iteration; r, the parameter is held in a constant ratio with the same parameter in another configuration; rs, the Slater parameters G^k, F^k held in a constant ratio with the corresponding parameter within the same configuration but with another k; p, the parameter fixed by $\zeta(d^2p) - \zeta(dsp) = \zeta(dsp) - \zeta(s^2p)$.

Parameter	Parameter values and associated standard errors for calculated subconfigurations (cm^{-1})		
	$4f^7 6s^2 6p$	$4f^7 5d6s6p$	$4f^7 5d^2 6p$
$A(d^2p)$			45 219(60)
$A(dsp)$		32 406(820)	
$A(s^2p)$	18 133(830)		
$T(^8S - {}^6P)$	32 000 f	32 000 f	32 000 f
$F^2(d,p)$		13 569(220)	7458(410)
$F^2(d,d)$			25 995(450)
$F^4(d,d)$			16 930(800)
$G^1(f,d)$		4 662(64)	6 496(90)
$G^3(f,d)$		6 294 rs	
$G^5(f,d)$		4 269 rs	
$G^2(f,p)$	1 297(180)	2 219(230)	2 704(180)
$G^4(f,p)$	1 400 rs	2 397 rs	
$G^1(d,p)$		8 475(140)	7 352(150)
$G^3(d,p)$		6 353 r	5 209(220)
$G^3(f,s)$		1 659(80)	
$G^2(d,s)$		4 473(280)	
$G^1(s,p)$		9 890(270)	
ζ_f	1 636(590)	1 636 r	
ζ_d		787(35)	568(32)
ζ_p	1 754 p	1 516(51)	1 278(78)
$\alpha_{L(L+1)}(d^2p)$			10 f
$\alpha_{L(L+1)}(dsp)$		10 f	

Configuration interaction parameter R^k (cm^{-1})

$4f^7 5d^2 6p - 4f^7 5d6s6p$	$R^2(dd,ds)$	= -8 480.53 f
$4f^7 5d^2 6p - 4f^7 5d6s6p$	$R^2(dp,sp)$	= -5 105 r
$4f^7 5d^2 6p - 4f^7 5d6s6p$	$R^1(dp,ps)$	= -5 139(840)
$4f^7 5d6s6p - 4f^7 6s^2 6p$	$R^2(dp,sp)$	= -5 745 r
$4f^7 5d6s6p - 4f^7 6s^2 6p$	$R^1(dp,ps)$	= -5 788 r
$4f^7 5d^2 6p - 4f^7 6s^2 6p$	$R^2(dd,ss)$	= 1 600 f

average percentage of the leading components:	60%
$\langle\overline{\delta E}\rangle$	165 cm^{-1}
rms deviation divided by the energy difference between the highest and lowest level:	0.57%

TABLE III. Leading eigenvector components for the investigated even-parity levels of Gd I, E_{obs}, g_{obs} according to [3]. $\mathcal{A} = {}^8S\ {}^9D\ {}^3P$, $\mathcal{B} = {}^8S\ {}^9D\ {}^1P$, $\mathcal{C} = {}^8S\ {}^7D\ {}^3P$, $\mathcal{D} = 4f^7({}^8S)6s^26p$; *obs*: observed, *calc*: calculated, $\Delta E = E_{obs} - E_{calc}$; a colon following a g_{obs} value indicates that it may be significantly less accurate than values given to the same number of decimal places but not so marked.

E_{obs} (cm^{-1})	E_{calc} (cm^{-1})	ΔE (cm^{-1})	g_{obs}	g_{calc}	J	Largest components	Contribution (%) of f^7s^2p	f^7dsp	f^7d^2p
16 885.739	16 879.446	96.293	1.88	1.884	5	85.88 % $\mathcal{A}\ {}^{11}D$ + 3.35 % $\mathcal{A}\ {}^{11}P$	0.01	99.93	0.06
17 318.942	17 494.532	-175.590	1.77	1.773	6	83.90 % $\mathcal{A}\ {}^{11}D$ + 4.61 % $\mathcal{A}\ {}^{9}D$	0.0	99.89	0.08
18 014.403	18 215.217	-200.814	1.70	1.704	7	90.04 % $\mathcal{A}\ {}^{11}D$ + 4.81 % $\mathcal{A}\ {}^{11}F$	0.0	99.97	0.01
17 227.969	17 178.802	49.167	3.33	3.339	1	62.78 % $\mathcal{A}\ {}^{9}F$ + 20.38 % $\mathcal{A}\ {}^{7}D$	0.0	99.81	0.17
17 380.827	17 345.645	35.182	2.105	2.123	2	56.16 % $\mathcal{A}\ {}^{9}F$ + 17.40 % $\mathcal{A}\ {}^{7}D$	5.04	94.69	0.25
17 617.767	17 584.823	32.944	1.79	1.791	3	55.33 % $\mathcal{A}\ {}^{9}F$ + 19.16 % $\mathcal{A}\ {}^{7}D$	1.96	97.84	0.20
17 973.611	17 945.165	28.446	1.69	1.665	4	51.45 % $\mathcal{A}\ {}^{9}F$ + 20.27 % $\mathcal{A}\ {}^{7}D$	0.53	99.22	0.16
18 509.198	18 502.127	7.071	1.61	1.606	5	48.33 % $\mathcal{A}\ {}^{9}F$ + 19.65 % $\mathcal{A}\ {}^{7}D$	0.05	99.76	0.20
17 749.978	17 545.701	204.277	2.606	2.633	2	74.51 % $\mathcal{A}\ {}^{9}D$ + 9.82 % $\mathcal{D}\ {}^{7}P$	10.16	88.53	1.27
17 795.267	17 648.942	146.325	2.076	2.084	3	80.63 % $\mathcal{A}\ {}^{9}D$ + 7.24 % $\mathcal{A}\ {}^{11}F$	0.77	97.93	1.27
17 930.516	17 775.738	154.778	1.83	1.867	4	74.01 % $\mathcal{A}\ {}^{9}D$ + 7.32 % $\mathcal{A}\ {}^{11}F$	0.12	98.64	1.20
18 070.257	17 890.965	179.292	1.71:	1.704	6	49.27 % $\mathcal{A}\ {}^{9}D$ + 19.66 % $\mathcal{A}\ {}^{11}P$	0.0	99.08	0.93
18 083.642	17 850.802	232.840	1.75:	1.766	5	60.72 % $\mathcal{A}\ {}^{9}D$ + 11.95 % $\mathcal{A}\ {}^{11}P$	0.14	98.75	1.06
23 103.660	23 350.679	-247.019	3.549:	3.437	1	67.15 % $\mathcal{B}\ {}^{9}F$ + 24.19 % $\mathcal{C}\ {}^{9}F$	0.0	99.23	0.76
23 215.028	23 420.696	-205.668	2.176:	2.136	2	64.00 % $\mathcal{B}\ {}^{9}F$ + 22.96 % $\mathcal{C}\ {}^{9}F$	0.10	99.09	0.75
23 389.782	23 557.125	-167.343	1.833	1.809	3	60.25 % $\mathcal{B}\ {}^{9}F$ + 21.15 % $\mathcal{C}\ {}^{9}F$	0.07	99.10	0.79
23 644.156	23 773.348	-129.192	1.696	1.681	4	55.41 % $\mathcal{B}\ {}^{9}F$ + 18.36 % $\mathcal{C}\ {}^{9}F$	0.02	99.13	0.82
23 999.912	24 069.602	-69.690	1.631	1.617	5	51.20 % $\mathcal{B}\ {}^{9}F$ + 15.10 % $\mathcal{C}\ {}^{9}F$	0.0	99.17	0.82
24 430.425	24 490.063	-59.638	1.580	1.580	6	43.28 % $\mathcal{B}\ {}^{9}F$ + 18.35 % $\mathcal{C}\ {}^{7}F$	0.0	98.99	0.99
25 376.313	25 156.654	219.659	1.58	1.568	7	69.82 % $\mathcal{B}\ {}^{9}F$ + 21.10 % $\mathcal{C}\ {}^{9}F$	0.0	99.54	0.45
24 458.988	24 239.675	219.313	2.31	2.403	2	53.94 % $\mathcal{A}\ {}^{7}P$ + 27.52 % $\mathcal{C}\ {}^{9}D$	4.24	95.55	0.17
24 849.514	24 854.865	-5.351	1.82	1.759	4	31.04 % $\mathcal{C}\ {}^{9}D$ + 24.88 % $\mathcal{B}\ {}^{9}D$	0.04	99.19	0.74
24 988.884	24 945.863	43.021	1.65	1.697	4	48.01 % $\mathcal{C}\ {}^{7}D$ + 22.48 % $\mathcal{B}\ {}^{9}D$	0.10	99.10	0.78
25 043.649	25 116.440	-72.791	1.65	1.715	5	56.52 % $\mathcal{B}\ {}^{9}D$ + 22.00 % $\mathcal{C}\ {}^{9}D$	0.14	98.83	0.98

relativistic correction factors [22, 23] in order to obtain an unambiguous solution. The parameters a^{10}_{5d} and a^{01}_{5d} as well as a^{10}_{6p} and a^{01}_{6p} were based upon a^{12}_{5d} and a^{12}_{6p}, respectively. Similarly b^{11}_{5d}, b^{13}_{5d}, and b^{11}_{6p} were referred to b^{02}_{5d} and b^{02}_{6p}. The following ratios calculated with the formulas of [22] were used:

$$a^{01}_{5d}/a^{12}_{5d} = 0.941\,64\,, \quad a^{10}_{5d}/a^{12}_{5d} = -0.018\,85\,,$$
$$a^{01}_{6p}/a^{12}_{6p} = 0.747\,74\,, \quad a^{10}_{6p}/a^{12}_{6p} = -0.074\,10\,,$$
$$b^{11}_{5d}/b^{02}_{5d} = -0.052\,68\,, \quad b^{13}_{5d}/b^{02}_{5d} = 0.309\,63\,,$$
$$b^{11}_{6p}/b^{02}_{6p} = -0.185\,94\,.$$

The remaining parameters a^{01}_{4f}, a^{12}_{4f}, and b^{11}_{4f} arise as a consequence of the allowance for a ${}^6P$ core of $4f^7$. Since its mixing with $4f^7({}^8S)$ is only minor, the corresponding angular coefficients for the magnetic dipole hfs interaction are all of the order of $10^{-3} - 10^{-2}\ \alpha^{10}_{4f}$. However, it turns out that the uncertainties of the experimental data render a safe determination of such a small effect, as represented by the parameters a^{01}_{4f} and a^{12}_{4f}, impossible. As a test we related a^{01}_{4f} to a^{12}_{4f} and made a five-parameter fit to the experimental A values which used two distinct parameters for the $4f$ shell: a^{10} and a^{12}. There was no stability of a^{12} against changes in the number of equations entering the fit. While its value was scattered in a range of 9 GHz, it hardly effected other parameters. Thus a^{12}_{4f} could not be determined and this only had a small influence on the quality of the fit. Therefore we eliminated a^{12}_{4f} by coupling it to a^{12}_{5d} via the corresponding spin-orbit constant ζ_{nl} taken from the fine structure making use of the semiempirical expression

$$\langle r^{-3}\rangle^{k_sk_l}_{nl} = \frac{F_{k_sk_l}(nl, Z_{\rm eff})\ \zeta_{nl}}{\alpha^2 hcRa_0^3\ Z_{\rm eff}(nl)\ H(l, Z_{\rm eff})} \tag{7}$$

and the formula (e.g., [1])

$$a^{k_sk_l}_{nl} = 2\kappa\mu_B \frac{\mu_I}{I}\langle r^{-3}\rangle^{k_sk_l}_{nl}\,,$$

$$\kappa = \begin{cases} 1 & \text{for } k_sk_l = 01, 12 \\ \frac{2}{3} & \text{for } k_sk_l = 10\,, \end{cases} \tag{8}$$

where μ_B and μ_I are the Bohr magneton and nuclear moment, I represents the nuclear spin quantum number, a_0 is the Bohr radius, R is the Rydberg constant, h is the Planck constant, α is the fs constant according to Sommerfeld, and c is the speed of light. $F_{k_sk_l}$ is the Casimir and $H(l, Z_{\rm eff})$ a relativistic correction factor [22, 23] with $Z_{\rm eff}(4f) = Z - 35$, $Z_{\rm eff}(5d) = Z - 11$ [24]. We obtained for Gd ($Z = 64$)

$$a^{12}_{4f} = 3.538\,78 a^{12}_{5d}\,.$$

The resulting influence on the a^{12}_{5d} should be small.

Only for the level at 17 749.978 cm^{-1} a significant contribution from $4f^76s^26p$ had to be considered by the introduction of further parameters $a^{10}_{4f}(s^2p)$, $a^{01}_{4f}(s^2p)$, $a^{12}_{4f}(s^2p)$, $a^{10}_{6p}(s^2p)$, $a^{01}_{6p}(s^2p)$, $a^{12}_{6p}(s^2p)$, $b^{11}_{4f}(s^2p)$, $b^{02}_{6p}(s^2p)$, and $b^{11}_{6p}(s^2p)$, where s^2p stands for $4f^76s^26p$ and dsp for $4f^75d6s6p$. Cross-configuration parameters are expected to be very small and were neglected in this analysis. Because just this one level is strongly perturbed by $4f^76s^26p$ it is not possible to determine all these additional parameter values in a least-squares fit. Hence they

were expressed through the corresponding parameters of the $4f^7 5d6s6p$ configuration by the relations involving the spin-orbit constants taken from Table II,

$$a_{nl}^{k_s k_l}(s^2p) = \frac{\zeta(s^2p)}{\zeta(dsp)} a_{nl}^{k_s k_l}(dsp) \ , \tag{9}$$

$$b_{nl}^{k_s k_l}(s^2p) = \frac{\zeta(s^2p)}{\zeta(dsp)} b_{nl}^{k_s k_l}(dsp) \ . \tag{10}$$

Expression (9) for the magnetic-dipole hfs can be deduced using (7) and (8). Equation (10) is based on the relation (e.g., [1])

$$b_{nl}^{k_s k_l} = e^2 Q_{nl} \langle r^{-3} \rangle_{nl}^{k_s k_l} \ , \ k_s k_l = 11, 13, 02 \ , \tag{11}$$

where e is the electron charge and Q_{nl} the shielded quadrupole moment [25] determined from optical spectroscopic measurements.

a_{4f}^{10} was left free in order to account for core polarization effects that are not explicitly taken care of in the effective operator formalism. The adjustable parameters in the fit were then a_{4f}^{10}, a_{5d}^{12}, a_{6s}^{10}, a_{6p}^{12}, b_{4f}^{11}, b_{5d}^{02}, and b_{6p}^{02}. Up to 34 basis states had to be summed up, considering

TABLE IV. Experimental and theoretical magnetic and electric hfs constants $A_{\rm expt}$, $B_{\rm expt}$ and $A_{\rm calc}$, $B_{\rm calc}$ for even-parity states of Gd I $4f^7 5d6s6p$. δA and δB are the differences between experimental and theoretical constants. $\mathcal{A}$, $\mathcal{B}$, $\mathcal{C}$ are defined as in Table III. Entries labeled by a dash yield excessive deviations δA and δB, assumed to be caused by mixing of close lying neighboring states.

Level E_o (cm^{-1})	Assignment	J	$^{155}A_{\rm expt}$ (MHz)	$^{155}A_{\rm calc}$ (MHz)	$\delta^{155}A$ (MHz)	$^{155}B_{\rm expt}$ (MHz)	$^{155}B_{\rm calc}$ (MHz)	$\delta^{155}B$ (MHz)
16 885.739	$\mathcal{A}$ ^{11}D	5	-111.18(24)	-110.21	-0.96	242(8)	232.81	9.68
17 318.942		6	-106(3)	-100.72	-5.28	290(8)	376.15	-
18 014.403		7	-109.7(2)	-105.44	-4.30	-53.9(6)	-58.11	4.16
17 227.969	$\mathcal{A}$ ^{9}F	1	265.4(1.8)	265.55	-0.16	76.75(77)	84.64	-7.89
17 380.827		2	72.88(26)	71.65	1.23	-328.58(66)	-326.30	-2.27
17 617.767		3	31.32(33)	32.16	-0.84	-393.7(1.5)	-389.87	-3.84
17 973.611		4	-5.36(49)	18.70	-	-282.2(7.5)	-290.22	7.99
18 509.198		5	6.00(12)	9.62	-3.62	-87.6(1.3)	3.81	-
17 749.978	$\mathcal{A}$ ^{9}D	2	-86.97(27)	-87.51	0.54	-22.0(1.2)	-29.79	7.76
17 795.267		3	-94.08(19)	-89.54	-4.54	154.1(4.5)	165.17	-11.05
17 930.516		4	-71.45(54)	-101.10	-	206.6(1.3)	205.18	1.38
18 070.257		6	-101.67(19)	-106.61	4.94	-61.0(6)	-51.29	-9.71
18 083.642		5	-98.50(14)	-109.04	10.54	108.7(2.0)	-8.45	-
23 103.660	$\mathcal{B}$ ^{9}F	1	136.3(1.0)	31.68	-	59(8)	114.04	-
23 215.028		2	28.4 (4)	6.35	-	-219(8)	-437.50	-
23 389.782		3	2.3 (4)	-1.83	4.13	-295(8)	-510.90	-
23 644.156		4	-7.6 (4)	-7.07	-0.53	-248(8)	-344.60	-
23 999.912		5	-10.6 (4)	-14.35	3.75	-78(8)	18.26	-
24 430.425		6	-41.5 (2)	-27.26	-	348(6)	535.57	-
25 376.313		7	-6.7 (4)	-5.08	-1.62	592(8)	1228.11	-
24 458.988	$\mathcal{A}$ ^{7}P	2	239.30(48)	81.10	-	-4.30(39)	-33.75	-
24 849.514	$\mathcal{C}$ ^{9}D	4	-39.9 (4)	-63.37	-	103(8)	233.15	-
24 988.884	$\mathcal{C}$ ^{7}D	4	38.1(2.5)	34.39	3.71	292(5)	166.88	-
25 043.649	$\mathcal{B}$ ^{9}D	5	-28.9 (4)	-21.02	-7.88	412(8)	217.93	-

Level E_o (cm^{-1})	Assignment	J	$^{157}A_{\rm expt}$ (MHz)	$^{157}A_{\rm calc}$ (MHz)	$\delta^{157}A$ (MHz)	$^{157}B_{\rm expt}$ (MHz)	$^{157}B_{\rm calc}$ (MHz)	$\delta^{157}B$ (MHz)
16 885.739	$\mathcal{A}$ ^{11}D	5	-145.8(3)	-144.87	-0.93	258(5)	247.99	10.34
17 318.942		6	-140(4)	-132.37	-7.63	309(8)	400.32	-
18 014.403		7	-143.9(2)	-138.37	-5.54	-57.5(6)	-61.58	4.11
17 227.969	$\mathcal{A}$ ^{9}F	1	347.1(4.1)	347.37	-0.26	80.1(1.7)	89.99	-9.89
17 380.827		2	95.64(44)	93.85	1.79	-350.3(2.3)	-346.96	-3.37
17 617.767		3	41.10(22)	42.40	-1.30	-418.0(2.0)	-414.49	-3.53
17 973.611		4	-7.00(62)	24.85	-	-300.5(7.6)	-309.05	8.59
18 509.198		5	7.81(11)	12.91	-5.10	-93.4(2.1)	4.27	-
17 749.978	$\mathcal{A}$ ^{9}D	2	-114.47(50)	-115.20	0.73	-23.6(1.4)	-31.69	8.09
17 795.267		3	-123.52(20)	-117.69	-5.83	163.8(4.3)	175.91	-12.13
17 930.516		4	-93.2(1.2)	-132.78	-	220.52(37)	218.51	2.02
18 070.257		6	-133.46(26)	-139.97	6.52	-64.93(85)	-54.71	-10.23
18 083.642		5	-129.32(12)	-143.13	13.81	115.2(2.5)	-9.02	-
23 103.660	$\mathcal{B}$ ^{9}F	1	147.6(1.0)	40.54	-	65(8)	121.24	-
23 215.028		2	38.0 (4)	8.08	-	-233(8)	-465.27	-
23 389.782		3	2.3 (4)	-2.41	4.71	-312(8)	-543.22	-
23 644.156		4	-9.2 (4)	-9.17	-0.03	-266(8)	-366.34	-
23 999.912		5	-13.6 (4)	-18.70	5.10	-80(8)	19.55	-
24 430.425		6	-54.4 (3)	-35.66	-	370(6)	569.70	-
25 376.313		7	-8.5 (4)	-6.54	-1.96	632(8)	1306.23	-
24 458.988	$\mathcal{A}$ ^{7}P	2	313.76(8)	106.39	-	-4.43(40)	-35.81	-
24 849.514	$\mathcal{C}$ ^{9}D	4	-52.5 (4)	-83.31	-	102(8)	248.15	-
24 988.884	$\mathcal{C}$ ^{7}D	4	50.1(3.0)	45.04	5.05	310(4)	177.07	-
25 043.649	$\mathcal{B}$ ^{9}D	5	-37.9 (4)	-27.62	-10.28	439(8)	232.08	-

mixing contributions as small as 0.01% for each fs level. The fit was carried out both for ^{155}Gd and ^{157}Gd.

V. RESULTS

The first fit attempts indicated that the inclusion of the seven levels for which in Table IV no differences δA between the experimental $A_{\rm expt}$ and theoretical $A_{\rm calc}$ hfs constants are given considerably reduces the fit quality. This suggests a lesser quality of the wave functions for these levels compared to that of all other levels. As a consequence these levels were excluded from the fit for the further analysis of the hfs. Consistent results for the one-electron dipole parameters with a rms deviation of 4.6 MHz for ^{155}A and 6.0 MHz for ^{157}A were obtained by solving the remaining system of 17 linear equations using the angular coefficients in intermediate coupling. In view of the complicated nature of the considered $4f^7 5d6s6p$ configuration and the great number of parameters, the fit to the A constants can be regarded as good. Table IV reveals a strong mutual mixing between the closely spaced states $\mathcal{A}\,^9F_4$ and $\mathcal{A}\,^9D_4$, which is not accounted for in the fine structure. The states $\mathcal{A}$, $\mathcal{B}$, and $\mathcal{C}$ are defined in the caption of Table III. The calculated value of -101.10 MHz for ^{155}A belonging to the level at 17 930.516 cm^{-1} lies below the experimental value of -71.45 MHz. This value can be raised by an admixture from $\mathcal{A}\,^9F$ of more than 0.16% — as it is now given by the fs calculation. Inversely, a greater percentage than 0.33% $\mathcal{A}\,^9D$ could reduce the discrepancy at 17 973.611 cm^{-1}. For the remaining five excluded levels mixing with other states not covered in Table I is likely. For example, the level $\mathcal{B}\,^9F_6$ at 24 430.425 cm^{-1} is certainly mixed with 24 854.297 cm^{-1} ($4f^8 5d6s\,^9G_6$ in the National Bureau of Standards Tables [3]). Both of them decay to the pure ^9D ground term of $4f^7 5d6s^2$. The intensity tables indicate stronger decay from 24 854.297 cm^{-1} than from 24 430.425 cm^{-1}. Since the transitions between pure $4f^8 5d6s$ and $4f^7 5d6s^2$ are not allowed, the approximation of the noninteracting $4f^8 5d6s$ and $4f^7(5d{+}6s)^2 6p$ groups fails here. In the case of the state $\mathcal{C}\,^9D_4$ at 24 849.514 cm^{-1} a $J = 3$ level only 10.526 cm^{-1} above exists [3]. Here at least, and for the states $\mathcal{B}\,^9F_1$ and $\mathcal{B}\,^9F_2$ separated by 111.368 cm^{-1}, the distortion of the measured hfs pattern caused by second-order hyperfine interactions might also be possible. That could be caused by a mixing of hyperfine states with the same quantum number F formed by neighboring fine-structure levels differing in J [26].

Similar to the magnetic-dipole parameters of the $4f$ shell, the coefficients of b^{11}_{4f} due to a weak $4f^7(^6P)$ admixture are also relatively small and with little changes throughout all levels considered. However, a coupling of them to those of $5d$ or $6p$ leads to a description of the observed $B_{\rm expt}$ factors with just two parameters, which is a too far-reaching reduction because the standard deviation increases considerably. Thus a fit to the $B_{\rm expt}$ factors with three parameters was performed, but only two parameters yielded reliable values. The rms standard deviation amounts to 7.7 MHz for ^{155}Gd and 8.5 MHz for ^{157}Gd. Unlike the case of the magnetic-dipole hyperfine interaction no large deviations were found for the constant B at $\mathcal{A}\,^9F_4$ and $\mathcal{A}\,^9D_4$ (see Table IV). In addition there is no obvious reason that an acceptable fit could only be made to the levels below 18 083.642 cm^{-1}. After all it can be stated that the sensitivity of any specific theoretical value $B_{\rm calc}$ to variations even in the least significant admixtures is considerably greater than in the case of the magnetic dipole interaction.

For a comprehensive comparison, our resulting one-electron hfs parameters are compiled in Table V together with those of other Gd I configurations. Unlike [2] where only a linear combination of the a_{10} parameters from the f, d, and s shell could be determined, we give the first isolated value of a^{10}_{6s}. For our parameters of the $6p$ shell there are also no comparative values available. The relativistic single-electron parameter can also be expressed in terms of the spin-orbit coupling constants, hence allowing a first assessment of their validity. With the nuclear dipole moment $\mu_I(^{155}\mathrm{Gd}) = -0.2567(6)\mu_n$ taken from [27], the quadrupole moment $Q(^{155}\mathrm{Gd}) = 1.30(2)b$ from

TABLE V. Relativistic one-electron hfs parameters (MHz) obtained from levels of the configurations $4f^7 5d6s^2$, $4f^7 5d^2 6s$, and $4f^7 5d6s6p$ of Gd I. Nonexistent parameters are denoted by -, existent but not yet determined ones by ⊔. The asterisk denotes values calculated from ^{157}Gd using the ratio $^{157}\mu/^{155}\mu = 1.311\,43(23)$ and $^{157}Q/^{155}Q = 1.065\,34(3)$ taken from [17].

	a^{10}_{4f}	a^{01}_{5d}	a^{12}_{5d}	a^{10}_{6s}	a^{12}_{6p}	Configuration		Reference
^{155}Gd	4.5(1.6)	⊔	-58(6)	-1270(22)	-68(17)	$4f^7 5d6s6p$		this work
		-38.9(4)	-13(4)	⊔	-	$4f^7 5d^2 6s$	$a\,^{11}F$	[2]
	2.6(1)	-44.9(4)	-22.2(15)	-	-	$4f^7 5d6s^2$	$a\,^9D$	[11]
	2.64(6)	-44.48(18)	-22.64(78)	-	-	$4f^7 5d6s^2$	$a\,^9D$	[17]
^{157}Gd	5.8(2.1)	⊔	-76(8)	-1668(28)	-88(22)	$4f^7 5d6s6p$		this work
		-51.0(5)	-17(5)	⊔	-	$4f^7 5d^2 6s$	$a\,^{11}F$	[2]
	3.3(1)	-58.4(4)	-30.2(17)	-	-	$4f^7 5d6s^2$	$a\,^9D$	[11]

	b^{02}_{5d}	b^{13}_{5d}	b^{11}_{5d}	b^{02}_{6p}	Configuration		Reference
^{155}Gd	1105(22)	⊔	⊔	1507(26)	$4f^7 5d6s6p$		this work
	974(28)	441(15)	-54(13)	-	$4f^7 5d^2 6s$	$a\,^{11}F$	[2]
	1064(3)	460(20)	-34(12)	-	$4f^7 5d6s^2$	$a\,^9D$	[11]
^{157}Gd	1175(24)	⊔	⊔	1603(29)	$4f^7 5d6s6p$		this work
	1038(30)	470(10)	-57(14)	-	$4f^7 5d^2 6s$	$a\,^{11}F$	[2]
	1135(3)	460(20)	-35(14)	-	$4f^7 5d6s^2$	$a\,^9D$	[11]

[28], nuclear spin $I = \frac{3}{2}$, and Eqs. (7), (8), and (11) one obtains

$$a_{4f}^{10} = 0.45 \text{ MHz}, \quad a_{5d}^{12} = -45 \text{ MHz},$$

$$a_{6p}^{12} = -102 \text{ MHz},$$

$$b_{5d}^{02} = 826 \text{ MHz}, \quad b_{6p}^{02} = 1421 \text{ MHz}.$$

As an estimate a_{6s}^{10} can be approximated by application of the empirical formula of Goudsmit-Fermi-Segrè according to [22]

$$a_{6s}^{10} = \frac{8}{3} R\alpha^2 Z_i \frac{Z_a^2}{n_a^3}\left(1 - \frac{d\Delta}{dn}\right) \times F_r(l=0, Z)(1-\delta)(1-\epsilon)\frac{m_e}{m_p}\frac{\mu_I}{I}, \tag{12}$$

where m_e/m_p is the electron-proton mass ratio. Z_i is the effective nuclear charge in the inner region and can be put equal to Z for an s electron. Z_a is the effective exterior charge and is taken to be equal 1 for the neutral atom. $\Delta = n - n_a$ reflects the quantum defect and n_a the effective principal quantum number. The value

$$\frac{Z_a^2}{n_a^3}\left(1 - \frac{d\Delta}{dn}\right) = 0.319$$

in Refs. [29, 30] is adopted. The Bohr-Weisskopf correction ϵ [31] for the extended nuclear magnetization in our case is given by $1 - \epsilon = 1.0145$. The precondition of a uniform distribution of the nuclear magnetization seems to be fulfilled, since the Gd nucleus contains a sufficient large number of protons. A nonpunctual distribution of the nuclear charge leads according to Crawford and Schawlow to a further correction $1 - \delta = 0.9441$ corresponding to a homogeneous charge density [32]. With the relativistic correction $F_r(l = 0, Z = 64) = 1.5946$ [22] we finally obtain for ^{155}Gd

$$a_{6s}^{10} = -1358 \text{ MHz}.$$

More recently, a refined calculation of the effect of the distributed nuclear charge on the magnetic-dipole hfs interaction between the nucleus and the atomic electron was presented by Rosenberg and Stroke [33]. This leads for ^{155}Gd to $1 - \delta = 0.9592$ and thus

$$a_{6s}^{10} = -1379 \text{ MHz}.$$

Assuming, as stated by Rosenberg and Stroke, that magnetic moment values calculated with the uniform and diffuse charge distributions differ as much as 5%, both values for the estimated hfs parameter a_{6s}^{10} are identical within this uncertainty of absolute 70 MHz. As further stated by Rosenberg and Stroke, the discrepancy between the experimental and calculated values may be as large as about 8%, i.e., in our case 110 MHz. Compared to the theoretical values the experimental one in Table V is in accord with the 8% assumption.

For the remaining parameters, sign and order of magnitude of the experimental values given for $4f^7 5d6s6p$ in Table V are well reproduced with the exception of a_{4f}^{10}. Here the fitted contact parameter is one order of magnitude greater, which demonstrates that besides purely relativistic influences it is predominantly caused through further effects. Since the analysis of the hfs in other elements revealed that the dominant contribution comes from core polarization [1] the underestimated value for a_{4f}^{10} might be such an effect. The trend for ^{157}Gd is very similar. The corresponding values may be obtained by multiplication by the isotopic ratios given at the bottom of Table V.

For the sake of comparison with other lanthanides we calculated from the set of data for ^{155}Gd the corresponding $\langle r^{-3}\rangle_{nl}^{k_s k_l}$ parameters using (8) and (11). In Fig. 3 they are shown systematically extending over the entire series of lanthanides taken from [1]. The present $\langle r^{-3}\rangle_{nl}^{k_s k_l}$ values lie well within the trend determined by those parameters which originate from configurations with one to three open electron shells. However, $\langle r^{-3}\rangle_{5d}^{12}$ originating from the spin-spin term clearly deviates. There is no obvious reason for this; a possible cause might be an influence of the ^6P core stemming from the coupling of the spin-orbit and spin-spin parameters of the $4f$ shell to a_{5d}^{12}. Apart from this the number of unfilled electron shells obviously does not influence the value of one-electron radial integrals. As already stated by Childs [2], the values found for the hfs radial integrals depend only slightly on the particular electron configuration from which they are evaluated (see, e.g., Table V).

VI. QUADRUPOLE MOMENT

The electric-quadrupole moment of the nuclear ground state can be derived from the hfs parameters a_{nl}^{12}, b_{nl}^{02} using (8), (11), and Casimir's relativistic correction factors $F_{k_s k_l}$, $R_{k_s k_l}$ according to

$$Q_{nl} = 2\frac{\mu_B}{e^2}\frac{\mu_I}{I}\frac{b_{nl}^{02}}{a_{nl}^{12}}\frac{F_{12}(nl, Z_{\text{eff}})}{R_{02}(nl, Z_{\text{eff}})}. \tag{13}$$

In the present analysis of the hfs, the quadrupole moment can be evaluated independently from the $5d$ ($F_{12} = 1.107\,452$, $R_{02} = 1.084\,997$) and $6p$ electron shells ($F_{12} = 1.691\,942$, $R_{02} = 1.255\,555$). In Table VI the results are given for ^{157}Gd together with the data from other authors. The antishielding factors R_{nl} for the $5d$ and $6p$ electrons were assumed to be as given in Ref. [34]. Our values obtained for the corrected quadrupole moment Q calculated from the $5d$ and $6p$ electron shell differ significantly. However, the correct order of magnitude is indicated by their mean. This strong deviation is certainly caused by configuration interaction which was only partially considered in the calculation of the wave functions used for the levels investigated. As pointed out in Refs. [1, 24], the a^{12} is especially sensitive. The effect of this can be clearly demonstrated using the set of parameters of $4f^7 5d6^2 6s$ from Childs [2] where for the $5d$ shell both a^{12} and a^{01} are given. Again, the calculation of Q involving a^{12} leads, with the value of $Q = 4.54(1.47)b$, to a great discrepancy compared to the remaining results

of Table VI, whereas a^{01} gives a consistent value. Hence the calculation of the quadrupole moment requires an individual evaluation of all three single-electron parameters $a_{nl}^{k_s k_l}$ for a given shell.

VII. CONCLUSION

The present work extends systematic studies of the hyperfine structure to a configuration with four distinct shells. A multiconfigurational fine-structure analysis for three configurations of Gd I ($4f^7 6s^2 6p$, $4f^7 5d6s6p$, and $4f^7 5d^2 6p$) was performed. In many cases, the separation between levels of the same J value is not much larger than the deviations between experimental and theoretical energies. This and the neglected mixing between $4f^8(^7F)5d6s$ and the studied group are two main reasons for limiting the quality of the eigenfunctions. Nevertheless, it served as a basis for the evaluation of the single-electron hfs constants a_{4f}^{10}, a_{5d}^{12}, a_{6s}^{10}, a_{6p}^{12}, b_{5d}^{02}, and b_{6p}^{02} for the even-parity configuration $4f^7 5d6s6p$. The corresponding effective $\langle r^{-3}\rangle$ values with one exception could be embedded into the trends established by data originating from configurations with one to three open electron shells. However, further experimental as well as

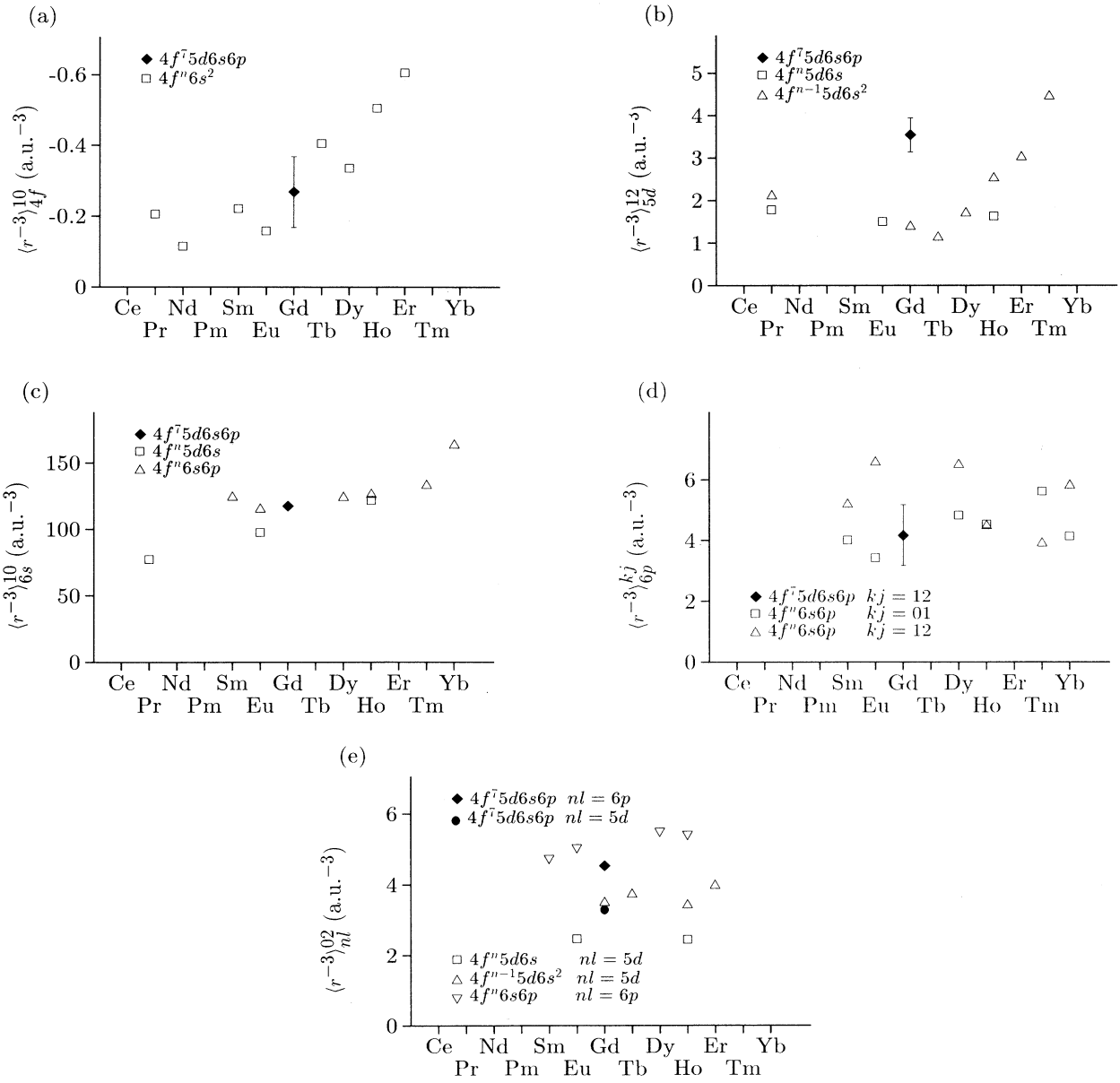

FIG. 3. Known experimental hyperfine radial intergrals $\langle r^{-3}\rangle_{nl}^{k_s k_l}$ in (a.u.$^{-3}$) for the lanthanides. For clarity their standard deviation is represented by error bars only for $4f^7 5d6s6p$. A missing bar indicates a standard deviation smaller than the size of the symbol.

TABLE VI. Nuclear quadrupole moment Q of ^{157}Gd in barns. Q_{nl} quadrupole moment before Sternheimer correction, R_{nl} Sternheimer antishielding factor. If more than one value is given its mean is taken (slanted). The asterisk denotes that the data for ^{155}Gd were obtained using the isotopic ratios as given in the caption of Table V. The dagger denotes values calculated from the data as given by Child [2].

Configuration	nl	Q_{nl} (b)	R_{nl}	$Q = Q_{nl}/(1 - R_{nl})$ (b)	Reference	Calculated using the hfs parameters
$4f^7 5d6s6p$	5d	1.44(18)	-0.25(5)	1.1547	this work	a^{12}, b^{02}
	6p	2.24(60)	-0.18(5)	1.9016	this work	a^{12}, b^{02}
				1.53(53)		
$4f^7 5d6s^2$	5d			1.36(6)	[11]	a^{01}, b^{02}
$4f^7 5d^2 6s$	5d	5.67(1.83)	-0.25(5)	4.54(1.47)	[2]†	a^{12}, b^{02}
	5d	1.78(7)	-0.25(5)	1.42(6)	[2]†	a^{01}, b^{02}
$4f^7 5d6s$	5d	1.65(16)	-0.25(5)	1.32(14)	[34]	a_{5d}, b_{5d}, nonrelativistic
$4f^7 5d6p$	5d	1.61(13)	-0.25(5)	1.19(12)	[34]	a_{5d}, b_{5d}, nonrelativistic
$4f^7 5d6p$	6p	1.63(13)	-0.18(5)	1.38(12)	[34]	a_{5d}, b_{5d}, nonrelativistic
				1.34(7)	[34]	
$4f^7 5d6s^2$	5d	1.69(17)	-0.25(5)	1.36(15)	[17]*	
				1.36(2)	[28]	muonic measurements

theoretical efforts appear to be necessary to obtain (i) an improved understanding of the J dependence of the B constants for highly excited levels, (ii) *ab initio* calculations for the $\langle r^{-3}\rangle_{nl}^{k_s k_l}$ integrals, especially for $\langle r^{-3}\rangle_{5d}^{12}$, and (iii) more detailed single-electron hfs parameter values, which, e.g., are a precondition for extracting reliable data for the quadrupole moment.

ACKNOWLEDGMENTS

A. Bachelier and J. Sinzelle are acknowledged for making the atomic structure calculation codes available to us. The calculations were performed on the CYBER 960-11 computer at Paris-Sud-Informatique.

APPENDIX

SL-limit expressions for the magnetic dipole (A) and electric quadrupole (B) hfs constants have been published for states of l^N, $l^N l'$, and $l_1^{N_1} l_2^{N_2} l_2^{N_2}$ configurations [2, 24], which all are based on the effective-operator technique of Sandars and Beck. The levels of the configuration $4f^7 5d6s6p$ considered in this work require a further generalization of the formulas given in [2]. We assume a two-stage coupling of four open shells, each denoted by

$$(n_i l_i)^{N_i} \alpha_i S_i L_i = \Psi_i \ , \tag{A1}$$

$(\Psi_1, \Psi_2)\Psi_{12}$, and $(\Psi_3, \Psi_4)\Psi_{34}$ to form the final SL-coupled state

$$|\,[(\Psi_1, \Psi_2)\Psi_{12}, (\Psi_3, \Psi_4)\Psi_{34}]\Psi_J\rangle$$

$$= |\,\{[(n_1 l_1)^{N_1} \alpha_1 S_1 L_1, (n_2 l_2)^{N_2} \alpha_2 S_2 L_2] S_{12} L_{12}, [(n_3 l_3)^{N_3} \alpha_3 S_3 L_3, (n_4 l_4)^{N_4} \alpha_4 S_4 L_4] S_{34} L_{34}\} SLJ\rangle \ . \tag{A2}$$

The evaluation of the diagonal matrix elements

$$\langle [(\Psi_1, \Psi_2)\Psi_{12}, (\Psi_3, \Psi_4)\Psi_{34}] SLJIFM \mid H_{hfs} \mid [(\Psi_1, \Psi_2)\Psi_{12}, (\Psi_3, \Psi_4)\Psi_{34}] SLJIFM\rangle \tag{A3}$$

yields the following expression for the magnetic-dipole hyperfine constant A of the state

$$\Psi = |\,[(l_1^{N_1} \alpha_1 S_1 L_1, l_2^{N_2} \alpha_2 S_2 L_2) S_{12} L_{12}, (l_3^{N_3} \alpha_3 S_3 L_3, l_4^{N_4} \alpha_4 S_4 L_4) S_{34} L_{34}] SLJ\,\rangle$$

adopting the convention $[\,j\,] = 2j + 1$ for any quantum number j:

$$A(\psi, \psi') = \sqrt{2J+1}/\sqrt{J(J+1)}$$

$$\times \Bigg(\delta(\alpha S, \alpha' S') \delta(L_1, L_1') \delta(L_2, L_2') \delta(L_3, L_3') \delta(L_4, L_4') (-1)^{(S+L'+J+1)} \sqrt{[L][L']} \begin{Bmatrix} J & J & 1 \\ L' & L & S \end{Bmatrix}$$

$$\times \Bigg[\delta(L_{34}, L_{34}') (-1)^{(L_{12}+L_{34}+L')} \sqrt{[L_{12}][L_{12}']} \begin{Bmatrix} L & L' & 1 \\ L_{12}' & L_{12} & L_{34} \end{Bmatrix}$$

$$
\times \left(a_1^{01}(-1)^{(L_1+L_2+L'_{12})} \begin{Bmatrix} L_{12} & L'_{12} & 1 \\ L_1 & L_1 & L_2 \end{Bmatrix} \sqrt{L_1(L_1+1)(2L_1+1)} \right.
$$

$$
\left. + a_2^{01}(-1)^{(L_1+L_2+L_{12})} \begin{Bmatrix} L_{12} & L'_{12} & 1 \\ L_2 & L_2 & L_1 \end{Bmatrix} \sqrt{L_2(L_2+1)(2L_2+1)} \right)
$$

$$
+ \delta(L_{12}, L'_{12})(-1)^{(L_{12}+L'_{34}+L)} \sqrt{[L_{34}][L'_{34}]} \begin{Bmatrix} L & L' & 1 \\ L'_{34} & L_{34} & L_{12} \end{Bmatrix}
$$

$$
\times \left(a_3^{01}(-1)^{(L_3+L_4+L'_{34})} \begin{Bmatrix} L_{34} & L'_{34} & 1 \\ L_3 & L_3 & L_4 \end{Bmatrix} \sqrt{L_3(L_3+1)(2L_3+1)} \right.
$$

$$
\left. \left. + a_4^{01}(-1)^{(L_3+L_4+L_{34})} \begin{Bmatrix} L_{34} & L'_{34} & 1 \\ L_4 & L_4 & L_3 \end{Bmatrix} \sqrt{L_4(L_4+1)(2L_4+1)} \right) \right]
$$

$$
+ \delta(\alpha L, \alpha' L') \delta(S_1, S'_1) \delta(S_2, S'_2) \delta(S_3, S'_3) \delta(S_4, S'_4) (-1)^{(S+L+J+1)} \sqrt{[S][S']} \begin{Bmatrix} J & J & 1 \\ S' & S & L \end{Bmatrix}
$$

$$
\times \left[\delta(S_{34}, S'_{34})(-1)^{(S_{12}+S_{34}+S')} \sqrt{[S_{12}][S'_{12}]} \begin{Bmatrix} S & S' & 1 \\ S'_{12} & S_{12} & S_{34} \end{Bmatrix} \right.
$$

$$
\times \left(a_1^{10}(-1)^{(S_1+S_2+S'_{12})} \begin{Bmatrix} S_{12} & S'_{12} & 1 \\ S_1 & S_1 & S_2 \end{Bmatrix} \sqrt{S_1(S_1+1)(2S_1+1)} \right.
$$

$$
\left. + a_2^{10}(-1)^{(S_1+S_2+S_{12})} \begin{Bmatrix} S_{12} & S'_{12} & 1 \\ S_2 & S_2 & S_1 \end{Bmatrix} \sqrt{S_2(S_2+1)(2S_2+1)} \right)
$$

$$
+ \delta(S_{12}, S'_{12})(-1)^{(S_{12}+S'_{34}+S)} \sqrt{[S_{34}][S'_{34}]} \begin{Bmatrix} S & S' & 1 \\ S'_{34} & S_{34} & S_{12} \end{Bmatrix}
$$

$$
\times \left(a_3^{10}(-1)^{(S_3+S_4+S'_{34})} \begin{Bmatrix} S_{34} & S'_{34} & 1 \\ S_3 & S_3 & S_4 \end{Bmatrix} \sqrt{S_3(S_3+1)(2S_3+1)} \right.
$$

$$
\left. \left. + a_4^{10}(-1)^{(S_3+S_4+S_{34})} \begin{Bmatrix} S_{34} & S'_{34} & 1 \\ S_4 & S_4 & S_3 \end{Bmatrix} \sqrt{S_4(S_4+1)(2S_4+1)} \right) \right]
$$

$$
+ \sqrt{30} \sqrt{[S][S'][L][L']} \begin{Bmatrix} S & S' & 1 \\ L & L' & 2 \\ J & J & 1 \end{Bmatrix}
$$

$$
\times \left[\delta(\alpha S_{34}, \alpha' S'_{34}) \delta(\alpha L_{34}, \alpha' L'_{34}) (-1)^{(S_{12}+S_{34}+S'+L_{12}+L_{34}+L')} \right.
$$

$$
\times \sqrt{[S_{12}][S'_{12}][L_{12}][L'_{12}]} \begin{Bmatrix} S & S' & 1 \\ S'_{12} & S_{12} & S_{34} \end{Bmatrix} \begin{Bmatrix} L & L' & 2 \\ L'_{12} & L_{12} & L_{34} \end{Bmatrix}
$$

$$
\times \left(a_1^{12} \delta(S_2, S'_2) \delta(L_2, L'_2) (-1)^{(S_1+S_2+S'_{12}+L_1+L_2+L'_{12})} \begin{Bmatrix} S_{12} & S'_{12} & 1 \\ S'_1 & S_1 & S_2 \end{Bmatrix} \begin{Bmatrix} L_{12} & L'_{12} & 2 \\ L'_1 & L_1 & L_2 \end{Bmatrix} \right.
$$

$$
\times \sqrt{\frac{l_1(l_1+1)(2l_1+1)}{(2l_1-1)(2l_1+3)}} \langle l_1^{N_1} \alpha_1 S_1 L_1 \parallel V^{(12)} \parallel l_1^{N_1} \alpha'_1 S'_1 L'_1 \rangle
$$

$$
+ a_2^{12} \delta(S_1, S'_1) \delta(L_1, L'_1) (-1)^{(S_1+S'_2+S_{12}+L_1+L'_2+L_{12})} \begin{Bmatrix} S_{12} & S'_{12} & 1 \\ S'_2 & S_2 & S_1 \end{Bmatrix} \begin{Bmatrix} L_{12} & L'_{12} & 2 \\ L'_2 & L_2 & L_1 \end{Bmatrix}
$$

$$
\left. \times \sqrt{\frac{l_2(l_2+1)(2l_2+1)}{(2l_2-1)(2l_2+3)}} \langle l_2^{N_2} \alpha_2 S_2 L_2 \parallel V^{(12)} \parallel l_2^{N_2} \alpha'_2 S'_2 L'_2 \rangle \right)
$$

$$
\begin{aligned}
&+ \delta(\alpha S_{12}, \alpha' S'_{12})\delta(\alpha L_{12}, \alpha' L'_{12})(-1)^{(S_{12}+S'_{34}+S+L_{12}+L'_{34}+L)} \\
&\times \sqrt{[S_{34}][S'_{34}][L_{34}][L'_{34}]} \begin{Bmatrix} S & S' & 1 \\ S'_{34} & S_{34} & S_{12} \end{Bmatrix} \begin{Bmatrix} L & L' & 2 \\ L'_{34} & L_{34} & L_{12} \end{Bmatrix} \\
&\times \left(a_3^{12}\delta(S_4, S'_4)\delta(L_4, L'_4)(-1)^{(S_3+S_4+S'_{34}+L_3+L_4+L'_{34})} \begin{Bmatrix} S_{34} & S'_{34} & 1 \\ S'_3 & S_3 & S_4 \end{Bmatrix} \begin{Bmatrix} L_{34} & L'_{34} & 2 \\ L'_3 & L_3 & L_4 \end{Bmatrix} \right. \\
&\times \sqrt{\frac{l_3(l_3+1)(2l_3+1)}{(2l_3-1)(2l_3+3)}} \langle l_3^{N_3} \alpha_3 S_3 L_3 \parallel V^{(12)} \parallel l_3^{N_3} \alpha'_3 S'_3 L'_3 \rangle \\
&+ a_4^{12}\delta(S_3, S'_3)\delta(L_3, L'_3)(-1)^{(S_3+S'_4+S_{34}+L_3+L'_4+L_{34})} \begin{Bmatrix} S_{34} & S'_{34} & 1 \\ S'_4 & S_4 & S_3 \end{Bmatrix} \begin{Bmatrix} L_{34} & L'_{34} & 2 \\ L'_4 & L_4 & L_3 \end{Bmatrix} \\
&\left. \times \sqrt{\frac{l_4(l_4+1)(2l_4+1)}{(2l_4-1)(2l_4+3)}} \langle l_4^{N_4} \alpha_4 S_4 L_4 \parallel V^{(12)} \parallel l_4^{N_4} \alpha'_4 S'_4 L'_4 \rangle \right) \Bigg] \Bigg) . \qquad \text{(A4)}
\end{aligned}
$$

Similarly we obtained for the electric-quadrupole hyperfine constant B:

$$
\begin{aligned}
&B(\psi, \psi') \\
&= 2\sqrt{J(2J-1)(2J+1)}/\sqrt{(J+1)(2J+3)} \\
&\times \left(\delta(\alpha S, \alpha' S')(-1)^{(S+L'+J)} \sqrt{[L][L']} \begin{Bmatrix} J & J & 2 \\ L' & L & S \end{Bmatrix} \right. \\
&\times \left[\delta(\alpha L_{34}, \alpha' L'_{34})(-1)^{(L_{12}+L_{34}+L')} \sqrt{[L_{12}][L'_{12}]} \begin{Bmatrix} L & L' & 2 \\ L'_{12} & L_{12} & L_{34} \end{Bmatrix} \right. \\
&\times \left(b_1^{02}\delta(L_2, L'_2)(-1)^{(L_1+L_2+L'_{12})} \begin{Bmatrix} L_{12} & L'_{12} & 2 \\ L'_1 & L_1 & L_2 \end{Bmatrix} \right. \\
&\times \sqrt{\frac{l_1(l_1+1)(2l_1+1)}{(2l_1-1)(2l_1+3)}} \langle l_1^{N_1} \alpha_1 S_1 L_1 \parallel U^{(2)} \parallel l_1^{N_1} \alpha'_1 S'_1 L'_1 \rangle \\
&+ b_2^{02}\delta(L_1, L'_1)(-1)^{(L_1+L'_2+L_{12})} \begin{Bmatrix} L_{12} & L'_{12} & 2 \\ L'_2 & L_2 & L_1 \end{Bmatrix} \\
&\left. \left. \times \sqrt{\frac{l_2(l_2+1)(2l_2+1)}{(2l_2-1)(2l_2+3)}} \langle l_2^{N_2} \alpha_2 S_2 L_2 \parallel U^{(2)} \parallel l_2^{N_2} \alpha'_2 S'_2 L'_2 \rangle \right) \right. \\
&+ \delta(\alpha L_{12}, \alpha' L'_{12})(-1)^{(L_{12}+L'_{34}+L)} \sqrt{[L_{34}][L'_{34}]} \begin{Bmatrix} L & L' & 2 \\ L'_{34} & L_{34} & L_{12} \end{Bmatrix} \\
&\times \left(b_3^{02}\delta(L_4, L'_4)(-1)^{(L_3+L_4+L'_{34})} \begin{Bmatrix} L_{34} & L'_{34} & 2 \\ L'_3 & L_3 & L_4 \end{Bmatrix} \right. \\
&\times \sqrt{\frac{l_3(l_3+1)(2l_3+1)}{(2l_3-1)(2l_3+3)}} \langle l_3^{N_3} \alpha_3 S_3 L_3 \parallel U^{(2)} \parallel l_3^{N_3} \alpha'_3 S'_3 L'_3 \rangle \\
&+ b_4^{02}\delta(L_3, L'_3)(-1)^{(L_3+L'_4+L_{34})} \begin{Bmatrix} L_{34} & L'_{34} & 2 \\ L'_4 & L_4 & L_3 \end{Bmatrix} \\
&\left. \left. \left. \times \sqrt{\frac{l_4(l_4+1)(2l_4+1)}{(2l_4-1)(2l_4+3)}} \langle l_4^{N_4} \alpha_4 S_4 L_4 \parallel U^{(2)} \parallel l_4^{N_4} \alpha'_4 S'_4 L'_4 \rangle \right) \right] \right.
\end{aligned}
$$

$$+\sqrt{[S][S'][L][L']}\begin{Bmatrix} S & S' & 1 \\ L & L' & 3 \\ J & J & 2 \end{Bmatrix}$$

$$\times\Bigg[\delta(\alpha S_{34},\alpha' S'_{34})\delta(\alpha L_{34},\alpha' L'_{34})(-1)^{(S_{12}+S_{34}+S'+L_{12}+L_{34}+L')}$$

$$\times\sqrt{[S_{12}][S'_{12}][L_{12}][L'_{12}]}\begin{Bmatrix} S & S' & 1 \\ S'_{12} & S_{12} & S_{34} \end{Bmatrix}\begin{Bmatrix} L & L' & 3 \\ L'_{12} & L_{12} & L_{34} \end{Bmatrix}$$

$$\times\Bigg(b_1^{13}\delta(S_2,S'_2)\delta(L_2,L'_2)(-1)^{(S_1+S_2+S'_{12}+L_1+L_2+L'_{12})}$$

$$\times\begin{Bmatrix} S_{12} & S'_{12} & 1 \\ S'_1 & S_1 & S_2 \end{Bmatrix}\begin{Bmatrix} L_{12} & L'_{12} & 3 \\ L'_1 & L_1 & L_2 \end{Bmatrix}\langle l_1^{N_1}\alpha_1 S_1 L_1 \parallel V^{(13)} \parallel l_1^{N_1}\alpha'_1 S'_1 L'_1\rangle$$

$$+ b_2^{13}\delta(S_1,S'_1)\delta(L_1,L'_1)(-1)^{(S_1+S'_2+S_{12}+L_1+L'_2+L_{12})}$$

$$\times\begin{Bmatrix} S_{12} & S'_{12} & 1 \\ S'_2 & S_2 & S_1 \end{Bmatrix}\begin{Bmatrix} L_{12} & L'_{12} & 3 \\ L'_2 & L_2 & L_1 \end{Bmatrix}\langle l_2^{N_2}\alpha_2 S_2 L_2 \parallel V^{(13)} \parallel l_2^{N_2}\alpha'_2 S'_2 L'_2\rangle\Bigg)$$

$$+\delta(\alpha S_{12},\alpha' S'_{12})\delta(\alpha L_{12},\alpha' L'_{12})(-1)^{(S_{12}+S'_{34}+S+L_{12}+L'_{34}+L)}$$

$$\times\sqrt{[S_{34}][S'_{34}][L_{34}][L'_{34}]}\begin{Bmatrix} S & S' & 1 \\ S'_{34} & S_{34} & S_{12} \end{Bmatrix}\begin{Bmatrix} L & L' & 3 \\ L'_{34} & L_{34} & L_{12} \end{Bmatrix}$$

$$\times\Bigg(b_3^{13}\delta(S_4,S'_4)\delta(L_4,L'_4)(-1)^{(S_3+S_4+S'_{34}+L_3+L_4+L'_{34})}$$

$$\times\begin{Bmatrix} S_{34} & S'_{34} & 1 \\ S'_3 & S_3 & S_4 \end{Bmatrix}\begin{Bmatrix} L_{34} & L'_{34} & 3 \\ L'_3 & L_3 & L_4 \end{Bmatrix}\langle l_3^{N_3}\alpha_3 S_3 L_3 \parallel V^{(13)} \parallel l_3^{N_3}\alpha'_3 S'_3 L'_3\rangle$$

$$+ b_4^{13}\delta(S_3,S'_3)\delta(L_3,L'_3)(-1)^{(S_3+S'_4+S_{34}+L_3+L'_4+L_{34})}$$

$$\times\begin{Bmatrix} S_{34} & S'_{34} & 1 \\ S'_4 & S_4 & S_3 \end{Bmatrix}\begin{Bmatrix} L_{34} & L'_{34} & 3 \\ L'_4 & L_4 & L_3 \end{Bmatrix}\langle l_4^{N_4}\alpha_4 S_4 L_4 \parallel V^{(13)} \parallel l_4^{N_4}\alpha'_4 S'_4 L'_4\rangle\Bigg)\Bigg]$$

$$+\sqrt{[S][S'][L][L']}\begin{Bmatrix} S & S' & 1 \\ L & L' & 1 \\ J & J & 2 \end{Bmatrix}$$

$$\times\Bigg[\delta(\alpha S_{34},\alpha' S'_{34})\delta(\alpha L_{34},\alpha' L'_{34})(-1)^{(S_{12}+S_{34}+S'+L_{12}+L_{34}+L')}$$

$$\times\sqrt{[S_{12}][S'_{12}][L_{12}][L'_{12}]}\begin{Bmatrix} S & S' & 1 \\ S'_{12} & S_{12} & S_{34} \end{Bmatrix}\begin{Bmatrix} L & L' & 1 \\ L'_{12} & L_{12} & L_{34} \end{Bmatrix}$$

$$\times\Bigg(b_1^{11}\delta(S_2,S'_2)\delta(L_2,L'_2)(-1)^{(S_1+S_2+S'_{12}+L_1+L_2+L'_{12})}$$

$$\times\begin{Bmatrix} S_{12} & S'_{12} & 1 \\ S'_1 & S_1 & S_2 \end{Bmatrix}\begin{Bmatrix} L_{12} & L'_{12} & 1 \\ L'_1 & L_1 & L_2 \end{Bmatrix}\langle l_1^{N_1}\alpha_1 S_1 L_1 \parallel V^{(11)} \parallel l_1^{N_1}\alpha'_1 S'_1 L'_1\rangle$$

$$+ b_2^{11}\delta(S_1,S'_1)\delta(L_1,L'_1)(-1)^{(S_1+S'_2+S_{12}+L_1+L'_2+L_{12})}$$

$$\times\begin{Bmatrix} S_{12} & S'_{12} & 1 \\ S'_2 & S_2 & S_1 \end{Bmatrix}\begin{Bmatrix} L_{12} & L'_{12} & 1 \\ L'_2 & L_2 & L_1 \end{Bmatrix}\langle l_2^{N_2}\alpha_2 S_2 L_2 \parallel V^{(11)} \parallel l_2^{N_2}\alpha'_2 S'_2 L'_2\rangle\Bigg)$$

$$
\begin{aligned}
&+ \delta(\alpha S_{12}, \alpha' S'_{12})\delta(\alpha L_{12}, \alpha' L'_{12})(-1)^{(S_{12}+S'_{34}+S+L_{12}+L'_{34}+L)} \\
&\times \sqrt{[S_{34}][S'_{34}][L_{34}][L'_{34}]} \begin{Bmatrix} S & S' & 1 \\ S'_{34} & S_{34} & S_{12} \end{Bmatrix} \begin{Bmatrix} L & L' & 1 \\ L'_{34} & L_{34} & L_{12} \end{Bmatrix} \\
&\times \Bigg(b_3^{11}\delta(S_4, S'_4)\delta(L_4, L'_4)(-1)^{(S_3+S_4+S'_{34}+L_3+L_4+L'_{34})} \\
&\quad \times \begin{Bmatrix} S_{34} & S'_{34} & 1 \\ S'_3 & S_3 & S_4 \end{Bmatrix} \begin{Bmatrix} L_{34} & L'_{34} & 1 \\ L'_3 & L_3 & L_4 \end{Bmatrix} \langle l_3^{N_3}\alpha_3 S_3 L_3 \parallel V^{(11)} \parallel l_3^{N_3}\alpha'_3 S'_3 L'_3\rangle \\
&\quad + b_4^{11}\delta(S_3, S'_3)\delta(L_3, L'_3)(-1)^{(S_3+S'_4+S_{34}+L_3+L'_4+L_{34})} \\
&\quad \times \begin{Bmatrix} S_{34} & S'_{34} & 1 \\ S'_4 & S_4 & S_3 \end{Bmatrix} \begin{Bmatrix} L_{34} & L'_{34} & 1 \\ L'_4 & L_4 & L_3 \end{Bmatrix} \langle l_4^{N_4}\alpha_4 S_4 L_4 \parallel V^{(11)} \parallel l_4^{N_4}\alpha'_4 S'_4 L'_4\rangle \Bigg) \Bigg] \Bigg) . \qquad \text{(A5)}
\end{aligned}
$$

[1] V. Pfeufer, Z. Phys. D **4**, 351 (1987).
[2] W. J. Childs, Phys. Rev. A **39**, 4956 (1989).
[3] *Atomic Energy Levels, The Rare Earth Elements*, Natl. Bur. Stand. Ref. Data Ser., Natl. Bur. Stand. (U.S.) Circ. No. 60, edited by W. C. Martin, R. Zalubas, and L. Hagan (U.S. GPO, Washington, DC, 1978).
[4] S. K. Borisov *et al.*, Zh. Eksp. Teor. Fiz. **93**, 1545 (1987) [Sov. Phys. — JETP **66**, 882 (1988)].
[5] H.-D. Kronfeldt, G. Klemz, and D.-J. Weber, Z. Phys. D **10**, 103 (1988).
[6] H. Niki *et al.*, Opt. Commun. **70**, 16 (1989).
[7] Yu. P. Gangrskii *et al.*, Opt. Spectrosc. **67**, 457 (1989).
[8] H.-D. Kronfeldt, G. Klemz, and D.-J. Weber, J. Phys. B **23**, 1107 (1990).
[9] S. B. Dutta, A. G. Martin, W. F. Rogers, and D. L. Clark, Phys. Rev. C **42**, 1911 (1990).
[10] M. Wakasugi *et al.*, J. Phys. Soc. Jpn. **59**, 2700 (1990).
[11] W. G. Jin *et al.*, Phys. Rev. A **42**, 1416 (1990).
[12] H.-D. Kronfeldt and G. Klemz, Z. Phys. D **18**, 131 (1991).
[13] T. Pramila, in *Optogalvanic Spectroscopy*, Proceedings of the Second International Meeting on Optogalvanic Spectroscopy and Allied Topics, edited by R. S. Stewart and J. E. Lawler, IOP Conf. Proc. No. 113 (Institute of Physics and Physical Society, Bristol, 1991), Vol. 10, Sec. 9, p. 197.
[14] J.-R. Kropp, H.-D. Kronfeldt, and R. Winkler, Z. Phys. A **321**, 57 (1985).
[15] Chain of computer programs AGENAC, ASSAC, DIAGAC, and GRAMAC for energy-level calculations following Racah methods by A. Bachelier, Y. Bordarier, and J. Sinzelle (unpublished).
[16] D. Ashkenasi, G. Klemz, and H.-D. Kronfeldt, in *Optogalvanic Spectroscopy* (Ref. [13]), p. 289.
[17] P. J. Unsworth, J. Phys. B **2**, 122 (1969).
[18] S. Nir, Ph. D. thesis, Hebrew University, Jerusalem, 1969 (unpublished).
[19] Th. A. M. van Kleef, J. Blaise, and J. F. Wyart, J. Phys. (Paris) **32**, 609 (1971).
[20] J. F. Wyart, J. Opt. Soc. Am. **68**, 197 (1978).
[21] P. G. H. Sandars and J. Beck, Proc. R. Soc. London, Ser. A **289**, 97 (1965).
[22] H. Kopfermann, *Nuclear Moments* (Academic, New York, 1958).
[23] H. Casimir, *On the Interaction between Atomic Nuclei and Electrons* (Teylers Tweede Genootshap XI, Harlem, 1936).
[24] W. J. Childs, Case Stud. At. Phys. **3**, 215 (1973).
[25] R. M. Sternheimer, Phys. Rev. **146**, 140 (1966).
[26] H.-D. Kronfeldt, D.-J. Weber, J. Dembczyński, and E. Stachowska, Phys. Rev. A **44**, 5737 (1991).
[27] J. M. Baker, G. M. Copland, and B. M. Wanklyn, J. Phys. C **2**, 862 (1969).
[28] Y. Tanaka *et al.*, Phys. Rev. Lett. **51**, 1633 (1983).
[29] D. R. Speck, Phys. Rev. **101**, 1725 (1956).
[30] P. Brix, Z. Phys. **132**, 579 (1952).
[31] A. Bohr, V. F. Weisskopf, Phys. Rev. **77**, 94 (1950).
[32] M. F. Crawford and A. L. Schawlow, Phys. Rev. **76**, 1310 (1949).
[33] H. J. Rosenberg and H. H. Stroke, Phys. Rev. A **5**, 1992 (1972).
[34] H. P. Clieves and A. Steudel, Z. Phys. A **289**, 361 (1979).